Published in final edited form as:

Nat Immunol. 2014 December ; 15(12): 1143–1151. doi:10.1038/ni.3027.

A central role for Notch in effector CD8+ T cell differentiation

Ronald A. Backer[1,7,8,9], **Christina Helbig**[1,7,9], **Rebecca Gentek**[1], **Andrew Kent**[2], **Brian J. Laidlaw**[3], **Claudia X. Dominguez**[3], **Yevan S. de Souza**[1], **Stella E. van Trierum**[4], **Ruud van Beek**[4], **Guus F. Rimmelzwaan**[4], **Anja ten Brinke**[5], **A. Marcel Willemsen**[6], **Antoine H. C. van Kampen**[6], **Susan M. Kaech**[3], **J. Magarian Blander**[2], **Klaas van Gisbergen**[7], and **Derk Amsen**[1,7]

[1]Department of Cell Biology and Histology, Biostatistics and Bioinformatics (KEBB), Academic Medical Center, Meibergdreef 15, 1105AZ, Amsterdam, The Netherlands [2]The Icahn School of Medicine at Mount Sinai, Immunology Institute and Tisch Cancer Institute, Department of Medicine, 1425 Madison Avenue, New York, NY 10029, USA [3]Department of Immunobiology and Howard Hughes Medical Institute, Yale University, School of Medicine, 300 Cedar St, New Haven, CT 06520, USA [4]Department of Viroscience, Erasmus Medical Center, Rotterdam, The Netherlands; Viroclinics Biosciences BV, Rotterdam, The Netherlands [5]Department of Immunopathology, 7Department of Hematopoiesis, Sanquin Research and Landsteiner Laboratory, Plesmanlaan 125, 1066 CX Amsterdam, The Netherlands [6]Bioinformatics Laboratory, Clinical Epidemiology, Biostatistics and Bioinformatics (KEBB), Academic Medical Center, Meibergdreef 15, 1105AZ, Amsterdam, The Netherlands [7]Department of Hematopoiesis, Sanquin Research and Landsteiner Laboratory, Plesmanlaan 125, 1066 CX Amsterdam, The Netherlands

Abstract

Activated CD8+ T cells choose between terminal effector cell (TEC) or memory precursor cell (MPC) fates. We show that Notch controls this choice. Notch promoted differentiation of immediately protective TECs and was correspondingly required for clearance of an acute influenza virus infection. Notch activated a major portion of the TEC-specific gene expression program and suppressed the MPC-specific program. Expression of Notch receptors was induced on naïve CD8+ T cells by inflammatory mediators and interleukin 2 (IL-2) via mTOR and T-bet dependent pathways. These pathways were subsequently amplified downstream of Notch, creating

Correspondence should be addressed to D.A. (D.amsen@sanquin.nl). Telephone +31 6 1093 27002826 6769, FAX +31 20 512 3474.
[8]current address: TRON Translationale Onkologie an der Universitätsmedizin der Johannes Gutenberg-Universität Mainz gGmbH, 55131 Mainz, Germany
[9]these authors contributed equally

ACCESSION CODES

Array Express (E-MTAB-2255)

AUTHOR CONTRIBUTIONS

R.A.B. designed, performed and analyzed experiments and wrote the manuscript. C.H., R.G., A.K., B.J.L., C.X.D., A.t.B., S.E.vT., R.v.B. and Y.S.d.S. performed and analyzed experiments, A.M.W. and A.H.C.v.K. analyzed RNAseq data, S.M.K., J.M.B., G.F.R. and K.v.G. designed and analyzed experiments. D.A. supervised the study, designed experiments and wrote the manuscript.

COMPETING FINANCIAL INTERESTS?

The authors have no competing financial interests.

a positive feedback loop. Notch thus functions as a central hub where information from different sources converges to match effector T cell differentiation to the demands of the infection.

Keywords

CD8 T cell; effector; memory; inflammation; MPC; TEC

The adaptive immune system must simultaneously curb the acute threat of microbial infections and generate immunological memory. Adaptive immunity to intracellular pathogens largely depends on $CD8^+$ T cells. Protective $CD8^+$ T cell responses require expansion of naive antigen-specific cells and their differentiation into cytolytic and cytokine-producing effector cells[1]. Different types of effector cells are generated, responsible for acute protection or generation of memory[1, 2]. At one extreme, a population of terminally differentiated $KLRG1^+CD127^-$ effector cells exists (terminal effector cells, TECs), which are mostly short-lived[1, 2]. The capacity to differentiate into long-lived memory cells is found predominantly in a $KLRG1^-CD127^+$ population, collectively referred to as memory precursor cells (MPCs)[1]. Apart from ability to survive, marked differences exist between these populations. TECs express higher amounts of effector molecules than MPCs[3] and favor migration to non-lymphoid tissues and splenic red pulp. In contrast, MPCs preferentially home to lymph nodes and splenic white pulp[4]. Both lineages express distinct transcriptional programs. The transcription factors Blimp1 and T-bet are critical regulators of the TEC gene expression program[2, 3, 5], whereas Eomesodermin, Tcf-1, FoxO1, Stat3 and Id3 control various aspects of MPC biology[6–12].

TECs and MPCs can derive from a single naive $CD8^+$ T cell or from different precursors[13]. Cells committed to either lineage can be identified among $KLRG1^-CD127^-$ early effector cells (EECs) within three days after infection[9, 14, 15]. An important question is how differentiating $CD8^+$ T cells choose between effector cell fates. This choice may be affected by asymmetric segregation of fate determining factors[16]. It stands to reason that generation of TECs is proportional to the severity of the infection[17]: greater infectious load requires generation of more fully armed effector cells, without increasing the demand for memory cells. Such proportionality would require instructive signals that relay information regarding the severity of infection. Candidates include inflammatory cytokines, such as interleukin 12 (IL-12) and type I interferons (IFN), help by $CD4^+$ T cells, and strong IL-2 receptor signaling, all of which promote generation of TECs[2, 14, 15, 18, 19]. Given the potentially harmful consequences from erroneous generation of highly cytotoxic TECs, it makes intuitive sense that their generation requires licensing by multiple signals.

The cell surface receptor Notch is a conserved regulator of binary cell fate decisions[20]. Notch responds to membrane bound ligands of the Delta-like (DLL) and Jagged families. Its intracellular domain (NICD) acts as a transcriptional activator after ligand induced cleavage and nuclear translocation[20]. All four mammalian Notch receptors activate a pathway involving recruitment to DNA via RBPJ molecules[21]. Notch reportedly regulates the gene encoding Eomesodermin, a factor required for the formation of stable $CD8^+$ T cell memory[10, 22]. Furthermore, during asymmetric division of naive $CD8^+$ T cells, an inhibitor

of Notch signaling called Numb is targeted towards the proximal cell, destined to become a TEC[16]. These findings suggest that Notch may promote MPC and inhibit TEC differentiation. On the other hand, *in vitro* experiments have implicated Notch in control of the genes encoding IFN-γ, Perforin, Granzyme B and T-bet[22–26], more consistent with a positive role in differentiation of TECs. To establish whether Notch governs the cell fate decision between TEC and MPC, we here used the well-characterized influenza virus infection model and mice with T cell specific genetic deficiencies in the Notch pathway. We find that Notch is an essential hub in a feed forward network to integrate multiple signal inputs and translate these into differentiation of fully protective TECs.

Results

TEC promoting signals induce Notch expression

To study how the degree of viral infection affects effector $CD8^+$ T cell differentiation, we infected mice intranasally with different concentrations of the A/HK×31 (HK×31) influenza strain.influenza strain. Influenza specific $CD8^+$ T cells were identified at the peak of the response (day 10-results not shown) using D^b tetramers loaded with the immunodominant 366–374 peptide of the influenza nucleoprotein (H-2 D^b–NP)[27]. Increasing viral loads across a 100-fold range resulted in great elevation of TEC numbers, whereas the number of MPCs remained constant (Fig. 1a). This result suggests that signals exist, which couple the severity of the infectious threat to generation of TECs.

To examine whether Notch could be involved in this process, we determined whether expression of Notch receptors on $CD8^+$ T cells is regulated by signals known to promote TEC differentiation. Important among these are inflammatory mediators produced by antigen presenting cells (APCs). We incubated naive $CD8^+$ T cells with dendritic cells (DCs) and added the RNA analog R-848, a mimic of RNA viruses. These conditions indeed induced surface expression of Notch1 on the naïve $CD8^+$ T cells within 24 h (Fig. 1b). Expression of Notch2 was only marginally induced. Addition of R-848 to naive $CD8^+$ T cells without DCs did not elevate expression of Notch1, but supernatant from DCs treated with R-848 (R-848 DC sup) did (Supplementary Fig. 1a and b). This induction required the presence of the TLR adapter Myd88 in DC, but not in T cells (Supplementary Fig. 1b and c). Lipopolysaccharide (LPS) similarly induced expression of Notch1 on naïve $CD8^+$ T cells via a Myd88-dependent pathway in DCs (Supplementary Fig. 1b). Thus, TLR activation stimulates DCs to produce soluble factors that in turn induce surface expression of Notch receptors on naïve $CD8^+$ T cells. Such soluble factors also elevated the expression of RBPJ mRNA (Fig. 1c), suggesting general enablement of the Notch pathway.

T cell receptor (TCR)-mediated activation of naive OT-I $CD8^+$ T cells by DCs presenting the Ovalbumin peptide (amino acids 257–264) resulted in modest induction of Notch1 and Notch2 (Fig. 1d). Induction of both these receptors was markedly enhanced by addition of R-848 (Fig. 1d). This induction was not due to improved antigen presentation, as R-848 DC supernatant also enhanced Notch1 expression on $CD8^+$ T cells activated with antibodies to CD3 (Fig. 1e).

To identify the soluble mediators responsible for induction of Notch, we focused on type I IFN. These cytokines are produced by APCs upon recognition of viral nucleic acids and promote differentiation of TECs[15, 19, 28]. $CD8^+$ T cells lacking expression of IFNAR1, the receptor for type I IFN, failed to elevate Notch1 in response to R-848 DC supernatant (Fig. 1f). Thus, $CD8^+$ T cells respond to type I IFN by elevating surface expression of Notch1.

We further tested whether signaling pathways known to regulate differentiation of TECs might control expression of Notch. The rapamycin-sensitive TORC1 complex is required for differentiation of TECs[29–31] and is activated by type I IFN receptor signaling[32]. Rapamycin almost abrogated induction of Notch1 expression on $CD8^+$ T cells by R-848 DC supernatant (Fig. 1g). Differentiation of TECs also depends on T-bet[2]. Expression of this factor was induced in naive $CD8^+$ T cells by R-848 DC supernatant (results not shown) and is partially responsible for induction of Notch1 expression, as Notch1 surface expression was reduced in *Tbx21*$^{-/-}$ T cells (Fig. 1h). Finally, strong IL-2 receptor signaling enhances TEC differentiation[14, 18] and IL-2 also synergized with TCR stimulation to elevate expression of Notch1 (Fig. 1i).

Consistent with a role in driving TEC differentiation, Notch abundance was also transiently elevated *in vivo* on early $KLRG1^+$ effector cells compared to $KLRG1^-$ effector cells (Supplementary Fig. 2). Thus, promoters of TEC differentiation also induce receptivity of the Notch pathway in $CD8^+$ T cells. Convergence of all these signals on expression of Notch suggests that perhaps Notch plays a role in guiding the decision between TEC and MPC differentiation.

Notch ligands are induced on APC by viral infection

Two major populations of APCs in lungs are $CD11c^{hi}MHCII^{int}$ alveolar macrophages and $CD11c^{high}MHCII^{high}$ migratory DC (characterized by intermediate and large size, respectively) (Fig. 2a, **middle** and Supplementary Fig. 3a)[33, 34]. These migratory DCs (mDCs) were shown to carry influenza antigen to the mediastinal lymph nodes and are responsible for priming naive $CD8^+$ T cells through direct presentation[34, 35]. Both mDCs and alveolar macrophages expressed undetectable amounts of Dll4 and Jagged2 and low amounts of Dll1 and Jagged1 in lungs from uninfected mice (Fig. 2a, bottom). Expression of Dll1 and Jagged1 was increased on both types of APCs upon infection with influenza virus (Fig. 2a, bottom). This elevated expression persisted on lung-derived migratory DCs (but not lymph node resident macrophages) isolated from the lung-draining mediastinal lymph nodes from infected mice (Fig. 2b and Supplementary Fig. 3b). Yet, Notch ligands were virtually undetectable on other populations of $MHCII^+$ cells present in lungs, even upon infection with influenza (Supplementary Fig. 3c). Therefore, expression of Notch ligands is induced by influenza infection on the APC that prime naive $CD8^+$ T cells, positioning these molecules for a potential role in differentiation of virus specific $CD8^+$ T cells.

Notch controls acquisition of effector function

The above results show that the Notch signaling module is assembled on both sides of the T cell-APC interface under conditions favoring differentiation of TECs. To investigate whether Notch controls differentiation of these cells, we used mice lacking expression of

Notch genes in the T cell lineage. Notch1 and Notch2 are both expressed in $CD8^+$ T cells (Fig. 1), whereas expression of Notch3 and Notch4 is undetectable[26]. We therefore generated mice lacking expression of both Notch1 and Notch2 by crossing a *Cd4*-Cre transgene with floxed alleles of the *Notch1* and *Notch2* genes. *Notch1*$^{flox/flox}$*Notch2*$^{flox/flox}$*Cd4*-Cre mice (Notch1-2-KO mice) lack expression of both Notch receptors in mature $CD4^+$ and $CD8^+$ T cells (results not shown). Thymic T cell development was not overtly affected in these mice[36].

Upon infection with HK×31, similar numbers of H-2 D^b–NP-binding $CD8^+$ T cells were found in blood, spleens or lungs from wild-type and Notch1-2-KO mice at the peak of the response (Fig. 3a–c). However, the proportion of influenza specific $CD8^+$ T cells was consistently higher in mediastinal lymph nodes from Notch1-2-KO than from wild-type mice (Fig. 3d). Also, Notch1-2-KO $CD8^+$ T cells preferentially localized to sites in spleens not accessible to antibodies injected into the blood stream, suggesting localization in the white pulp (Fig. 3e)[37]. Although the proportion of IL-2 producing cells in response to $NP_{366–374}$ peptide was similar between wild-type and Notch1-2-KO $CD8^+$ effector T cells, production of IFN-γ or tumor necrosis factor (TNF) were reduced in the latter (Fig. 3f). Production of the cytolytic effector molecule granzyme B was almost undetectable in Notch1-2-KO $CD8^+$ T cells and mRNA abundance for both granzyme B and perforin were reduced in these cells (Fig. 3g). Low expression of these molecules translated into reduced cytolytic effector function in an *in vivo* cytolysis assay. Whereas nearly all $CFSE^{lo}$ NP peptide–loaded splenocytes were killed by pre-infected wild-type mice, a proportion of peptide carrying cells could still be detected in infected Notch1-2-KO mice (Fig. 3h). As expected from these defects in effector function, viral clearance and weight recovery were compromised in Notch1-2-KO mice infected with the aggressive A/PR/8/34 influenza strain (Fig. 3i,j). Although Notch1-2-KO mice also lack expression of Notch in $CD4^+$ T cells, defective viral clearance in these mice was not caused by ineffective help to B cells, as titers of neutralizing antibodies to A/PR/8/34 were similar in both wild-type and Notch1-2-KO mice (Fig. 3k). Thus, Notch is required for generation of fully functional $CD8^+$ effector T cells.

Notch controls differentiation of TECs

High expression of effector molecules and residence outside lymph nodes and splenic white pulp are characteristics of TECs. In contrast, MPCs preferentially localize inside these locations and tend to exclusively produce IL-2 (refs.[3, 4, 37]). Our results are therefore consistent with a defect in the TEC compartment and an increase in MPCs in Notch1-2-KO mice. Indeed, hardly any $KLRG1^+CD127^-$ $CD8^+$ TEC T cells were detectable in Notch1-2-KO mice at the peak of the response, whereas numbers of $KLRG1^-CD127^+$ $CD8^+$ MPC T cells were increased (Fig. 4a). TECs were also absent in Notch1-2-KO mice at earlier and later time points, demonstrating that their absence did not reflect altered response kinetics (Fig. 4b). Partial loss of TECs was observed in mice lacking expression of only Notch1 or Notch2 (Fig. 4c) or mice that were heterozygous for both these genes (Supplementary Fig. 4). These results show that *Notch1* and *Notch2* act redundantly and that the presence of TECs is sensitive to Notch gene dosage. Furthermore, TECs were virtually non-existent when the canonical Notch effector RBPJ was deleted in T cells (Fig. 4d and Supplementary

Fig. 5). Dependence on Notch was not unique to the response to HK×31, as no TECs were detectable after infection with the A/PR/8/34 influenza strain (Supplementary Fig. 6).

To test whether defective development of KLRG1^{+}CD127^{-} CD8^{+} T cells in Notch1-2-KO mice depends on a direct role for Notch in CD8^{+} T cells, we generated mixed bone marrow chimeras and infected these with HK×31 influenza. Notch deficiency did not affect the efficacy of reconstitution (data not shown). However, CD45.2^{+} Notch1-2-KO CD8^{+} T cells failed to produce KLRG1^{+}CD127^{-} CD8^{+} T cells even in the presence of CD45.1^{+} wild-type cells (Fig. 4e,f), showing that TEC differentiation depends on a CD8^{+} T cell intrinsic role for Notch. Likewise, physiological numbers of Notch1-2-KO OT-I TCR transgenic CD8^{+} T cells failed to generate TECs after transfer into mice infected with the WSN-OVA$_{I}$ influenza strain, which expresses the H2K^{b}-restricted OVA$_{257–264}$ peptide (Supplementary Fig. 7). These data show that Notch controls TEC development in a CD8^{+} T cell–intrinsic manner and independent of influenza strain and TCR specificity.

As developmental defects could potentially indirectly perturb TEC differentiation in Notch1-2-KO mice, we inactivated Notch1 and Notch2 expression in mature CD8^{+} T cells. To this end, we retrovirally introduced Cre recombinase in *Notch1*$^{flox/flox}$*Notch2*$^{flox/flox}$ OT-I CD8^{+} T cells and transferred these into mice infected with the WSN-OVA$_{I}$ influenza strain (for full expansion *in vivo*-results not shown). Expression of Cre abrogated development of KLRG1^{+} cells (Fig. 4g). Vice versa, introduction of NICD1, the constitutively active intracellular domain of Notch1, restored the ability of Notch1-2-KO OT-I T cells to generate KLRG1^{+} cells (Fig. 4h). We conclude that Notch1 and Notch2 act directly in mature CD8^{+} T cells to drive the development of cells phenotypically resembling TECs.

Notch controls the gene expression signature of TECs

To examine whether Notch is required for adoption of full TEC identity, we determined the global gene expression profiles of Notch1-2-KO and wild-type CD8^{+} effector cells by whole transcriptome RNA sequencing. To this end, H-2 D^{b}–NP$_{366–374}$ binding CD8^{+} T cells were sorted by flow cytometry from mice infected with HK×31 influenza 10 days earlier. This population consists for well over 99% pure effector cells, as evidenced by their CD44^{+} phenotype (data not shown).

Gene set enrichment analysis for immunological signatures was performed, using the c7 gene set from the Molecular Signature Database (http://www.broadinstitute.org/gsea/msigdb/), to obtain an unbiased view of the types of processes affected by Notch deficiency. Consistent with a role for Notch in control of TEC differentiation, nine of the top ten most significantly enriched gene sets pertained to CD8^{+} effector T cell differentiation in general (labeled in yellow in Supplementary data set S1), and differentiation of TECs and MPCs in both viral and bacterial models in particular (labeled in red in Supplementary data set 1).

To more specifically determine whether the TEC program is controlled by Notch, we generated molecular definitions of TECs and MPCs by whole transcriptome sequencing of sorted KLRG1^{-}CD127^{+} and KLRG1^{+}CD127^{-} H-2 D^{b}–NP specific CD8^{+} T cell populations from wild-type mice. We found 132 TEC specific genes, whereas another 250 genes were preferentially expressed in MPCs (Supplementary data set 2). Assignment of these identities

to the genes with differential expression between wild-type and Notch1-2-KO H-2 D^b–NP specific $CD8^+$ T cells showed that a large proportion of Notch dependent genes (higher in wild-type) was TEC specific (labeled in green in Fig. 5a). Indeed, more than 40% of the TEC specific transcriptome was reduced in Notch1-2-KO $CD8^+$ effector T cells (green bar on left - Fig. 5b). Conversely, less than 2% of MPC genes were reduced in Notch1-2-KO $CD8^+$ effector T cells (magenta bars - Fig. 5b). Instead, expression of a large proportion (36%) of MPC specific genes was elevated (magenta in Fig. 5a,b). These results strongly suggest that Notch promotes TEC fate and may inhibit formation of MPCs.

As Notch controls expression of many, but not all, TEC signature genes (Fig. 5b), we examined whether Notch selectively controls specific functional categories. To this end, a side by side analysis was made of the Gene Ontology (GO) terms (Biological Pathways) enriched in the comparison of the wild-type versus Notch1-2-KO transcriptome and those enriched in the comparison of the MPC versus TEC transcriptome. We focused on the major functional categories, which define the difference between MPCs and TECs, including those associated with effector function, migration, viability, activation and differentiation (Fig. 5c). The near complete overlap of enriched Gene Ontology terms (shown by the red color of both the core and periphery of each node) revealed a representation of Notch-dependent genes in all these categories (Fig 5c). Thus, Notch does not control individual aspects of TEC differentiation, but exerts broad control throughout the TEC gene expression program. This conclusion was further supported by a comparison of the relative expression patterns of specific genes encoding transcription factors (involved in effector cell differentiation), chemokine receptors, adhesion molecules, cytotoxic effector molecules or Killer Lectin-like Receptors. Expression of TEC-specific genes across all these categories was reduced in Notch1-2-KO effector cells (Figs. 5d–i and Supplementary data set 3, compare expression ratios of MPC/TEC in dark blue and knock out/wild-type in light blue). Although some genes were either unaffected or only weakly affected, no TEC gene was significantly elevated in Notch1-2-KO effector cells. Reciprocally, expression of MPC specific genes was generally elevated in Notch1-2-KO effector cells or unchanged, but never reduced (Figs. 5d–i). Together, these results clearly show that Notch is a major regulator of the decision between TEC and MPC differentiation.

Notch feeds back onto TEC promoting pathways

Early TECs are characterized by high expression of CD25 (the IL-2 receptor α chain) and IL-2 receptor signaling promotes differentiation of TECs[14, 18]. CD25 is induced on $CD8^+$ T cells by constitutively active Notch[38], suggesting that this IL-2 receptor component is a downstream target of Notch. Indeed, expression of *Il2ra* mRNA was reduced in Notch1-2-KO effector $CD8^+$ T cells (Fig. 6a) as was CD25 expression on Notch1-2-KO OT-I $CD8^+$ T cells at early stages of the response (Fig. 6b), when differentiation takes place.

The Akt-mTOR pathway, an important regulator of TEC differentiation[29–31, 39, 40], is activated by IL-2 receptor signaling and functions downstream of Notch in thymocytes and T cell leukemia[41, 42]. We therefore examined whether Notch controls activity of this pathway during $CD8^+$ T cell responses. Activation of Akt requires phosphorylation of the 3-phosphoinositide-dependent kinase 1 (PDK1) substrate site T308 and this modification

positively correlates with high CD25 expression in early $CD8^+$ effector T cells *in vivo*[39, 40]. Phosphorylation of Akt T308 was clearly detectable in OT-I effector cells isolated from mice five days after infection with WSN-OVA_I influenza (Fig. 6c, top). In contrast, in Notch1-2-KO OT-I T cells, phosphorylation of this residue was reduced to background found in unactivated $CD44^-CD8^+$ T cells (Fig. 6c, top bar graph). Similar results were obtained for Akt-mediated phosphorylation of mTOR (S2448) and Foxo1/3 (Thr24/Thr32), which were both reduced to background in Notch1-2-KO OT-I cells (Fig. 6c, bottom bar graph; Supplementary Fig. 8a). Of note, expression of constitutively active Akt[41] in Notch1-2-KO OT-1 T cells was sufficient to restore differentiation of a $KLRG1^+$ population (Fig. 6d). These results support the conclusion that the Akt-mTOR pathway functions downstream of Notch in differentiation of TECs.

T-bet is an important transcriptional regulator of TEC development[2] (Fig. 6e). The *Tbx21* gene (encoding T-bet) is a direct target of Notch in $CD4^+$ T cells[24, 25] and correspondingly, the abundance of *Tbx21* mRNA was also reduced in Notch1-2-KO effector $CD8^+$ T cells (Fig. 6f). Genetic deficiency for T-bet largely abrogated the ability of retrovirally expressed NICD1 to induce development of $KLRG1^+$ effector $CD8^+$ T cells (Fig. 6g), whereas ectopic expression of T-bet restored differentiation of such cells in Notch1-2-KO effector $CD8^+$ T cells (Fig. 6h). These results strongly suggest that T-bet is a downstream effector of Notch in driving differentiation of TECs.

In conclusion, expression of the IL-2 receptor α chain and T-bet as well as activity of Akt and mTOR all depend on Notch. As these factors also act upstream of Notch by inducing its expression on naïve $CD8^+$ T cells (Fig. 1), these results show that Notch functions as a central hub in a network, which integrates signal input from different sources (inflammation, IL-2, Notch ligands) to induce generation of TECs (Supplementary Fig. 8b).

Discussion

How activated $CD8^+$ T cells decide between committing to the memory or the terminal effector cell lineage represents an intriguing conceptual question with implications for the vaccine design. Important is the requirement to balance effective rejection of invading microorganisms and the risk of immunopathology. Given their destructive potential, generation of TECs must be regulated by signals that shape the response to the threat posed by the infection. Indeed, inflammatory signals promote the development of TECs[2, 15, 17, 19]. We now show that Notch bridges signaling by innate pattern recognition receptors and inflammation to TEC development. Type I IFN induce expression of Notch receptors and RBPJ on $CD8^+$ T cells, while TLR and inflammatory cytokines induce expression of Notch ligands on APC[43, 44]. Thus, microbial and inflammatory stimuli activate both sides of the T cell-APC interface to assemble the Notch signaling module. Notch receptors and ligands never reach very high surface levels. However, it is important to note that these levels are often actively kept low, for instance by internalization[45, 46], a property that may promote dosage sensitivity of the pathway[47]. TEC differentiation is indeed sensitive to Notch dose, as shown in mice lacking *Notch1* or *Notch2* genes individually or heterozygous mice for both. Importantly, combined induction of receptors, ligands and the downstream mediator RBPJ likely results in cumulative amplification of signal amplitude.

Our results show that Notch, IL-2 receptor, mTOR and T-bet together form a positive feedback module, which integrates signals from various sources. These signals may signify the detection of living microorganisms (type I IFN), direct interaction of the APC with those micro-organisms (Notch ligands) and perhaps help by $CD4^+$ T cells (IL-2). Such a system requiring integration of multiple signals is presumably less prone to spuriously develop the potentially destructive TECs than one depending on an individual signal. Together, these factors (and possibly yet others) could serve as a licensing code, which allows full differentiation of TECs only when justified by the severity of the infection. The fact that delivery of all these signals together sets up a positive feedback loop, presumably ensures maximal separation between the TEC and MPC fates.

Notch and Akt promote survival in multiple cell types[48,49], but this does not appear to explain their roles in effector $CD8^+$ T cells. Activation of Akt in fact reduces survival of $CD8^+$ effector T cells *in vivo*, presumably by promoting differentiation of the short lived TEC fate[39, 50]. Likewise, our results are not consistent with a major role for Notch in survival of TECs. First, Notch deficiency does not affect the magnitude of the H-2 D^b–$NP_{366–374}$ specific response, inconsistent with loss of a major population. Second, if Notch deficiency compromised TEC survival, one would expect loss of the entire TEC signature in Notch1-2-KO mice. Instead, we find that approximately half of the TEC gene expression signature is unaffected by N1/2 deficiency. Furthermore, there are marked differences in the degree to which different TEC genes are affected. These data strongly suggest that Notch controls TEC differentiation by regulating a large proportion of the TEC specific gene expression program. In this program, some genes rely more heavily on Notch than others. Yet, in the absence of Notch, the program as a whole collapses, resulting in a severe differentiation defect. Direct Notch target genes have been identified with dedicated roles in effector $CD8^+$ T cells. These include the genes encoding granzyme B, perforin, IFN-γ and T-bet[22, 24–26]. Furthermore, Notch controls expression of a critical component of the IL-2 receptor as well as the amplitude of Akt and mTOR signaling during effector CD8 T cell differentiation. All of these promote differentiation of effector $CD8^+$ T cells and regulate additional transcription factors involved in this process, including STAT5, Foxo and HIF1 proteins[7, 39, 40, 51–53]. Thus, besides directly regulating key effector genes, Notch mobilizes additional signaling pathways and thereby coordinates an extensive differentiation program. Still, the fact that approximately half the TEC specific transcriptome is unaffected by the absence of Notch shows that the TEC differentiation program is modular. It seems likely that the other module(s) are controlled by additional signals activated by inflammation.

Loss of part of the TEC signature in Notch1-2-KO mice is mirrored by elevation of roughly a third of the MPC specific transcriptome. This unlikely reflects a relative increase in MPC numbers due to the absence of TECs, as that would result in elevation of the entire MPC transcriptome. The simplest interpretation of these data is therefore that, apart from inducing a TEC gene expression program, Notch represses part of the MPC program. This program may further be suppressed by additional TEC promoting signals and/or may require provision of MPC promoting signals, such as Wnts and activators of STAT3, including IL-10 and IL-21 (refs.[6, 11, 12]). Nonetheless, our results do suggest that avoiding (strong)

Notch signals is a condition to allow differentiation into the MPC lineage. How and where this condition exists during an infection will be an important question for future research.

Methods

Mice

All mice were on a C57BL/6 background.

Notch1$^{flox/flox}$*Notch2*$^{flox/flox}$*Cd4*-Cre mice or *Rbpj*$^{flox/flox}$*Cd4*-Cre mice were used[36, 43]. Cre-negative littermates were used in all experiments. Transgenes for the OT-I TCR (003831), P14 TCR (004694) as well as knock out mice for Myd88 (009088), IFNAR1 (032045) and Rag1 (002216) are all available from Jackson Laboratories. Mice were bred and housed in specific pathogen-free conditions at the Animal Centers of the Academic Medical Center (AMC, Amsterdam, The Netherlands), Mount Sinai School of Medicine (New York, NY, USA) and Yale University, School of Medicine (New Haven, CT, USA). Mice (both male and female) were between 8–16 weeks of age at the start of the experiment. During infection experiments, wild-type and Notch1-2-KO mice were housed together to avoid cage bias. No intentional method for randomization was used. No formal method for blinding was used, except for determination of viral loads and hemagglutination assay, where the operator did not know mouse genotypes. Mixed-bone marrow (BM) chimeras containing wild-type and Notch1-2-KO BM at a 1:1 ratio were generated via intravenous injection of 5–10 × 10^6 donor BM cells into lethally irradiated RAG1-deficient mice. Wild-type and Notch1-2-KO cells of donor origin were identified with the congenic CD45.1/2 markers. BM chimeras were used at 12 weeks after engraftment. All mice were used in accordance of institutional and national animal experimentation guidelines. All procedures were approved by the local Animal Ethics Committees.

Media, reagents and mAbs

Culture medium was Iscove's modified Dulbecco's medium (IMDM; Lonza) supplemented with 10% heat-inactivated FCS (Lonza), 200 U/ml penicillin, 200 μg/ml streptomycin (Gibco), GlutaMAX (Gibco) and 50 μM β-mercaptoethanol (Invitrogen) (IMDMc). All directly conjugated monoclonal antibodies used for flow cytometry were purchased from eBioscience, San Diego, CA, unless stated otherwise: anti-CD3ε (clone 145-2C11), anti-CD4 (clone GK1.5), anti-CD8α (Ly-2, clone 53-6.7), anti-CD8b (Ly-3, clone eBio341), anti-CD25 (anti-IL2Rα, clone 7D4), anti-CD28 (clone 37.51), anti-CD44 (clone IM7), anti-CD45.1 (clone A20, BD Biosciences), anti-CD45.2 (clone 104), anti-CD62L (clone MEL-14), anti-CD69 (clone H1.2F3), anti-CD127 (anti-IL7Rα, clone A7R34), anti-DLL1 (clone HMD1-5), anti-DLL4 (clone HMD4-1), anti-Granzyme B (clone GB-11, Sanquin PeliCluster), anti-IL-2 (clone JES6-5H4), anti-IFN-γ (clone XMG1.2), anti-Jagged1 (clone HMJ1-29), anti-Jagged2 (clone HMJ2-1), anti-KLRG-1 (clone 2F1), anti-Notch1 (clone HMN1-12, Biolegend), anti-Notch2 (clone HMN2-35, biolegend) and anti-TNFα (clone MP6-XT22), anti-p-AKT [T308] (cat. # 13038) and p-mTOR [S2448] (cat. # 5536), anti-FoxO1/3 [T24/T32] (cat.# 2599S); isotype control (cat. #3900S) (Cell Signaling Technology).

Influenza infection

Mice were intranasally infected with 100–200 × 50% tissue culture effective dose ($TCID_{50}$) of the H3N2 influenza A virus HK×31[27], influenza A/WSN/33, A/WSN/33–OVA(I)[54], A/PR/8/34 (H1N1) or the recombinant A/PR/8/34 expressing the LCMV $gp_{33–41}$ epitope[55]. Stocks and viral titers were obtained by infecting MDCK or LLC-MK2 cells as described previously[56].

At indicated time intervals, blood samples were drawn from the tail vein or mice were sacrificed and organs were collected to determine numbers of influenza-specific $CD8^+$ T cells. Influenza-specific $CD8^+$ T cells were enumerated using anti-CD8 (53-6.7) and PE- or APC-conjugated tetramers of $H\text{-}2D^b$ containing the influenza-A-derived nucleocapsid protein (NP) peptide $NP_{366–374}$ ASNENMETM (produced at the Sanquin Laboratory for Blood Research). A/PR/8/34 viral loads in lungs of infected mice were determined by isolating lung mRNA and detection of viral mRNA by quantitative PCR using the following primers and probe specific for the A/PR/8/34 M gene. Sense primer: 5’-CAAAGCGTCTACGCTGCAGTCC-3’; antisense primer: 5’-TTTGTGTTCACGCTCACCGTGCC-3’; Probe: 5’-AAGACCAATCCTGTCACCTCTGA-3’.

Sera were tested for the presence of neutralizing antibodies to this virus by hemagglutination inhibition (HI) assay as described previously using four hemagglutinating units of virus and turkey erythrocytes[57]. Values represent the maximum serum dilution at which agglutination was completely inhibited.

In vitro $CD8^+$ T cell activation

Single cell suspensions were prepared by grinding organs over 70 μm nylon sieves (BD Biosciences). Contaminating red blood cells were removed by hypotonic lysis (155 mM NH_4Cl, 10 mM $KHCO_3$, and 1 mM EDTA), and cell counts were determined by an automated cell counter (CasyCounter, Innovatis). $CD8^+$ T cell purification from spleen and peripheral lymph nodes was performed by MACS in accordance with manufacturer’s directions (Miltenyi Biotec) and naïve $CD44^-CD62L^+$ $CD8^+$ T cells were sorted by flow cytometry. To activate $CD8^+$ T cells *in vitro*, cells were cultured for 16–18 h in the presence of indicated concentrations of OVA-protein and CD11c-MACS purified splenic DCs (T:DC ratio was 1:1) or plate bound anti-CD3 (145-2C11) and soluble anti-CD28 (37.51) (50,000 T cells/well in 96-well plate). BMDC-conditioned supernatant was generated by stimulating GM-CSF–derived BMDCs in the absence or presence of 10 μg/ml R-848 or 100 ng/ml LPS. After overnight culture, BMDC-conditioned supernatant was isolated, centrifuged and passed through a 0.45 μM filter to remove remaining BMDCs and added to $CD8^+$ T cell cultures for 16–18 h.

Dendritic cell flow cytometry

Single cell suspensions were prepared by cutting lungs into small fragments followed by enzymatic digestion. For this, 1 ml IMDMc with 100U/ml collagenase type IV (Sigma-Aldrich) was added per lung lobe for 60 min incubation at 37 °C. Cold IMDMc containing 10 mM EDTA and 20 mM HEPES pH 7.5 was then added, and cells were filtered though 70

μm nylon sieves (BD Biosciences). Red blood cells were lysed by hypotonic lysis. Fc-receptors were blocked with anti-CD16/CD32 for 30 min, followed by staining DC- and macrophage-subsets with a cocktail of mAbs specific to CD11c, CD11b and MHC class II (I-A/I-E) and the different Notch ligands (for clone identifiers see at list of mAbs above).

Flow cytometry and cell sorting

For intracellular cytokine and granzyme B staining, splenocytes and total lung samples were stimulated with 1 μg/ml of the MHC class I restricted influenza-derived peptide $NP_{366–374}$ ASNENMETM for 4 h in the presence of 10 μg/ml brefeldin A (Sigma) to prevent cytokine release. Cells were stained with the relevant fluorochrome-conjugated mAbs for 30 min at 4 °C in PBS containing 0.5% BSA and 0.02% NaN_3. For intracellular staining, cells were fixed and permeabilized using the Cytofix/Cytoperm (BD Biosciences). For Phospho-specific flow cytometry, cells were fixed and permeabilized using Phosflow lysis and Phosflow PermWash I reagents (BD Biosciences) according to the manufacturer's recommendations and subsequently stained with the phosphor-specific antibodies for 1 h at 20°C. When required, cells were washed and additionally incubated with secondary antibody (Goat anti-Rabbit ALEXA488) for 40 min. Data acquisition and analysis was done on a FACSCanto (Becton Dickinson) and FlowJo software.

To isolate H-2 Db–NP tetramer-positive $CD8^+$ T cells from influenza infected mice, single cell suspensions of spleens were stained with influenza-specific tetramers and various markers. Cells were sorted using FACSAria cell sorters (BD Biosciences).

To discriminate between circulating T cells and T cells in splenic white pulp intravascular $CD8^+$ T cells were stained by injecting 1 μg anti-CD8β-PE (eBio341) i.v. 8 min before the animals were sacrificed. Organs were processed as described above, and $CD8^+$ T cells were stained *in vitro* with a different, noncompeting anti-CD8α antibody (53-6.7) along with antibodies to other surface markers.

Retroviral transductions and adoptive transfers of $CD8^+$ T cells

Virus was produced in PlatE cells as described[43]. Total splenocytes from $CD45.2^+$ OT-I wild-type or OT-I Notch1-2-KO mice were incubated with 1 nM $OVA_{257–264}$ peptide, and next day cells were spin-infected (700 × *g* for 90 min at 37°C) with viral supernatant (with 8 μg/ml polybrene), followed by 5 h at 37°C. Medium was replaced and next day, live T cells were isolated by density centrifugation (Lymphoprep, Axis-shield PoC) and between 7.5×10^2 and 5×10^4 cells (as indicated in Figure legends) were transferred into timed influenza-OVA infected $CD45.1^+$ mice. Donor OT-1 T cells were detected 5–10 days after transfer as $CD45.2^+CD8^+$ and Thy1.1 or GFP triple positive cells.

In vivo cytotoxicity assay

Target spleen cells from C57BL/6 mice were pulsed with 1 μg/ml influenza-derived peptide $NP_{366–374}$ for 35 min and subsequently labeled with 0.2 μM CFSE (Invitrogen) for 15 min at 37 °C ($CFSE^{low}$, specific target cells) or were not pulsed with peptide and labeled with 2 μM CFSE ($CFSE^{high}$, non-specific target cells). The two target populations were mixed in equal numbers and 5×10^6 cells were transferred i.v. into mice that had been infected with

influenza A virus HK×31 10 d before or into untreated control mice. Mice were killed 4 h later and the ratio between peptide-loaded versus empty target cells was quantified by flow cytometry.

Gene expression profiling

H-2 D^b–$NP_{366–374}{}^+CD8^+$ T cells were isolated from spleens of influenza infected mice by flow cytometry. Total RNA was extracted with TRIzol reagent (Invitrogen) according to the manufacturer's protocol. For Deep sequencing analysis, total RNA was further purified by nucleospin RNAII columns (Macherey-Nagel) and RNA was amplified using the Superscript RNA amplification system (Invitrogen) and labeled with the ULS system (Kreatech), using either Cy3 or Cy5 dyes (Amersham). Sequences were obtained by pooling 10 samples in one lane on a HiSeq2000 machine. Between 17 and 27 million reads were obtained per sample.

Read mapping (TopHat) and determining differentially expressed genes (DESeq) was done as described in[58]. Reads were mapped against the mouse reference genome (build mm9) using TopHat (version 1.4.0), which allows to span exon-exon junctions. TopHat was supplied with a known set of gene models (NCBI build 37, version 64). In order to obtain per sample genecounts HTSeq-count was used. This tool generates genecounts for each gene that is present in the provided Gene Transfer Format (GTF) file. Genes that have zero counts across all samples were removed from the dataset. Statistical analysis was performed using the R package DESeq. Differentially expressed genes were determined between the SLEC and MPEC samples, and between the wild type and knock-out samples. DESeq assumes that gene counts can be modelled by a negative binomial distribution. For sample normalisation the 'size factors' were determined from the count data. The empirical dispersion was determined with the 'pooled' method, which used the samples from all conditions with replicates to estimate a single pooled dispersion value. Subsequently, a parametric fit determines the dispersion-mean relationship for the expression values resulting in two dispersion estimates for each gene (the empirical estimated, and the fitted value). Using the 'maximum sharingMode' we selected the maximum of these two values to be more conservative. Finally, p-values and FDR corrected p-values were calculated.

To highlight biological processes that are over-represented in the set of differentially expressed genes we used Bioconductor package GOseq[59], which was developed for the analysis of RNA-seq data. First we selected all genes with an FDR<0.5 from the SLEC-MPEC and WT-KO comparisons. Subsequently, the GO 'Biological Processes' gene sets were used to determine over-represented processes. In addition we used the 'C7' gene set from the Molecular Signatures Database (MSigDB; http://www.broadinstitute.org/gsea), which is a collection of annotated gene sets. Gene set C7 comprises immunologic signatures composed of gene sets that represent cell types, states, and perturbations within the immune system. The signatures were generated by manual curation of published microarray studies in human and mouse immunology. This gene set was generated as part of the Human Immunology Project Consortium (HIPC; http://www.immuneprofiling.org). An in-house R script was developed to convert the C7 gene set into a format that could be used by GOseq.

To visualize the results for the GOseq analysis based on the GO biological processes, we used the Cytoscape Enrichment Map plugin[60]. We first constructed a gmt file containing the GO terms and corresponding ensembl gene identifiers. GO terms associated with more than 250 genes were removed because these represent too general terms that are difficult to interpret. In addition, very small gene sets (<15 genes) were removed because these are more likely to become significant by chance alone. Subsequently, from the results of the GOseq analysis we selected biological processes related to chemokines, cytokines, cytotoxicity, differentiation, adhesion, migration, apoptosis, activation and proliferation. Selected GO terms with FDR<0.5 were visualized as an enrichment map. RNAseq data can be accessed at Array Express (E-MTAB-2255)

Quantitative RT-PCR

cDNA was made with Oligo (dT) and random hexamers using the First Strand cDNA synthesis kit (Fermentas). Quantitative PCR using SYBRgreen (Bio-Rad) was performed using the C1000 Thermal Cycler (Bio-Rad). Relative concentrations were determined by normalizing to β-actin using the Bio-Rad CFX Manager software. Melt curves ensured amplification of a single product. Sequences of primers used: β-actin (5'-GAAGTCCCTCACCCTCCCAA-3' and 5'-GGCATGGACGCGACCA-3'), RBPJ (5'-CGGTCTGCTTATCAACTTTCC-3' and 5'-ATTCACAGTCCGAGATGGCTA-3'), Tbx21 (5'-CAACAACCCCTTTGCCAAAG-3' and 5'- TCCCCCAAGCAGTTGACAGT-3')

Statistical analysis

Figures represent means and error bars denote standard error of the mean (s.e.m.). Standard Student's *t*-tests (unpaired, two-tailed) was applied with GraphPadPrism software. If 3 or more groups were compared One-way ANOVA with Bonferroni correction was used. $P < 0.05$ was considered statistically significant.

Supplementary Material

Refer to Web version on PubMed Central for supplementary material.

ACKNOWLEDGEMENTS

We thank W. Pear (University of Pennsylvania), J.C. Zuniga Pflucker (Sunnybrook Research Institute) and D. Vignali (University of Pittsburgh) for expression constructs, T.N.M. Schumacher (Netherlands Cancer Institute) for influenza-Ova, J. den Haan (Free University of Amsterdam) for Myd88 deficient mice and M. Suresh and E.H. Kim (University of Wisconsin-Madison) for advice on phospho stainings. M. Wolkers, M. Nolte, R. van Lier and M. van Ham are acknowledged for helpful suggestions and proof reading of the manuscript. Furthermore, we acknowledge the NIH tetramer facility for providing MHC-tetramers. This study was supported by grants from NWO-ALW, the Landsteiner Foundation for Blood Research and an AMC fellowship to D.A. JMB is supported by NIH grants AI095245, DK072201, the Burroughs Wellcome Trust Fund, the Leukemia and Lymphoma Society, and the Irma-Hirschl and Monique Weill-Caulier Charitable Trust Funds

References

1. Kaech SM, Cui W. Transcriptional control of effector and memory CD8+ T cell differentiation. Nat Rev Immunol. 2012; 12:749–761. [PubMed: 23080391]
2. Joshi NS, et al. Inflammation directs memory precursor and short-lived effector CD8(+) T cell fates via the graded expression of T-bet transcription factor. Immunity. 2007; 27:281–295. [PubMed: 17723218]

3. Rutishauser RL, et al. Transcriptional repressor Blimp-1 promotes CD8(+) T cell terminal differentiation and represses the acquisition of central memory T cell properties. Immunity. 2009; 31:296–308. [PubMed: 19664941]
4. Jung YW, Rutishauser RL, Joshi NS, Haberman AM, Kaech SM. Differential localization of effector and memory CD8 T cell subsets in lymphoid organs during acute viral infection. J Immunol. 2010; 185:5315–5325. [PubMed: 20921525]
5. Kallies A, Xin A, Belz GT, Nutt SL. Blimp-1 transcription factor is required for the differentiation of effector CD8(+) T cells and memory responses. Immunity. 2009; 31:283–295. [PubMed: 19664942]
6. Cui W, Liu Y, Weinstein JS, Craft J, Kaech SM. An interleukin-21-interleukin-10-STAT3 pathway is critical for functional maturation of memory CD8+ T cells. Immunity. 2011; 35:792–805. [PubMed: 22118527]
7. Rao RR, Li Q, Gubbels Bupp MR, Shrikant PA. Transcription factor Foxo1 represses T-bet-mediated effector functions and promotes memory CD8(+) T cell differentiation. Immunity. 2012; 36:374–387. [PubMed: 22425248]
8. Ji Y, et al. Repression of the DNA-binding inhibitor Id3 by Blimp-1 limits the formation of memory CD8+ T cells. Nat Immunol. 2011; 12:1230–1237. [PubMed: 22057288]
9. Yang CY, et al. The transcriptional regulators Id2 and Id3 control the formation of distinct memory CD8+ T cell subsets. Nat Immunol. 2011; 12:1221–1229. [PubMed: 22057289]
10. Intlekofer AM, et al. Effector and memory CD8+ T cell fate coupled by T-bet and eomesodermin. Nat Immunol. 2005; 6:1236–1244. [PubMed: 16273099]
11. Zhou X, et al. Differentiation and persistence of memory CD8(+) T cells depend on T cell factor 1. Immunity. 2010; 33:229–240. [PubMed: 20727791]
12. Gattinoni L, et al. Wnt signaling arrests effector T cell differentiation and generates CD8+ memory stem cells. Nat Med. 2009; 15:808–813. [PubMed: 19525962]
13. Rohr JC, Gerlach C, Kok L, Schumacher TN. Single cell behavior in T cell differentiation. Trends Immunol. 2014; 35:170–177. [PubMed: 24657362]
14. Kalia V, et al. Prolonged interleukin-2Ralpha expression on virus-specific CD8+ T cells favors terminal-effector differentiation in vivo. Immunity. 2010; 32:91–103. [PubMed: 20096608]
15. Obar JJ, et al. Pathogen-induced inflammatory environment controls effector and memory CD8+ T cell differentiation. J Immunol. 2011; 187:4967–4978. [PubMed: 21987662]
16. Chang JT, et al. Asymmetric T lymphocyte division in the initiation of adaptive immune responses. Science. 2007; 315:1687–1691. [PubMed: 17332376]
17. Badovinac VP, Porter BB, Harty JT. CD8+ T cell contraction is controlled by early inflammation. Nat Immunol. 2004; 5:809–817. [PubMed: 15247915]
18. Obar JJ, et al. CD4+ T cell regulation of CD25 expression controls development of short-lived effector CD8+ T cells in primary and secondary responses. Proceedings of the National Academy of Sciences of the United States of America. 2010; 107:193–198. [PubMed: 19966302]
19. Wiesel M, et al. Type-I IFN drives the differentiation of short-lived effector CD8+ T cells in vivo. European journal of immunology. 2012; 42:320–329. [PubMed: 22102057]
20. Bray SJ. Notch signalling: a simple pathway becomes complex. Nat Rev Mol Cell Biol. 2006; 7:678–689. [PubMed: 16921404]
21. Kopan R, Ilagan MX. The canonical Notch signaling pathway: unfolding the activation mechanism. Cell. 2009; 137:216–233. [PubMed: 19379690]
22. Cho OH, et al. Notch regulates cytolytic effector function in CD8+ T cells. J Immunol. 2009; 182:3380–3389. [PubMed: 19265115]
23. Kuijk LM, et al. Notch controls generation and function of human effector CD8+ T cells. Blood. 2013; 121:2638–2646. [PubMed: 23380742]
24. Minter LM, et al. Inhibitors of gamma-secretase block in vivo and in vitro T helper type 1 polarization by preventing Notch upregulation of Tb×21. Nat Immunol. 2005; 6:680–688. [PubMed: 15991363]
25. Bailis W, et al. Notch simultaneously orchestrates multiple helper T cell programs independently of cytokine signals. Immunity. 2013; 39:148–159. [PubMed: 23890069]

26. Maekawa Y, et al. Notch2 integrates signaling by the transcription factors RBP-J and CREB1 to promote T cell cytotoxicity. Nat Immunol. 2008; 9:1140–1147. [PubMed: 18724371]
27. Belz GT, Xie W, Altman JD, Doherty PC. A previously unrecognized H-2D(b)-restricted peptide prominent in the primary influenza A virus-specific CD8(+) T-cell response is much less apparent following secondary challenge. J Virol. 2000; 74:3486–3493. [PubMed: 10729122]
28. Akira S, Hemmi H. Recognition of pathogen-associated molecular patterns by TLR family. Immunol Lett. 2003; 85:85–95. [PubMed: 12527213]
29. Pearce EL, et al. Enhancing CD8 T-cell memory by modulating fatty acid metabolism. Nature. 2009; 460:103–107. [PubMed: 19494812]
30. Rao RR, Li Q, Odunsi K, Shrikant PA. The mTOR kinase determines effector versus memory CD8+ T cell fate by regulating the expression of transcription factors T-bet and Eomesodermin. Immunity. 2010; 32:67–78. [PubMed: 20060330]
31. Araki K, et al. mTOR regulates memory CD8 T-cell differentiation. Nature. 2009; 460:108–112. [PubMed: 19543266]
32. Platanias LC. Mechanisms of type-I- and type-II-interferon-mediated signalling. Nat Rev Immunol. 2005; 5:375–386. [PubMed: 15864272]
33. Helft J, et al. Cross-presenting CD103+ dendritic cells are protected from influenza virus infection. J Clin Invest. 2012; 122:4037–4047. [PubMed: 23041628]
34. Lambrecht BN, Hammad H. Lung dendritic cells in respiratory viral infection and asthma: from protection to immunopathology. Annu Rev Immunol. 2012; 30:243–270. [PubMed: 22224777]
35. Braciale TJ, Sun J, Kim TS. Regulating the adaptive immune response to respiratory virus infection. Nat Rev Immunol. 2012; 12:295–305. [PubMed: 22402670]
36. Amsen D, et al. Direct regulation of Gata3 expression determines the T helper differentiation potential of Notch. Immunity. 2007; 27:89–99. [PubMed: 17658279]
37. Olson JA, McDonald-Hyman C, Jameson SC, Hamilton SE. Effector-like CD8(+) T cells in the memory population mediate potent protective immunity. Immunity. 2013; 38:1250–1260. [PubMed: 23746652]
38. Adler SH, et al. Notch signaling augments T cell responsiveness by enhancing CD25 expression. J Immunol. 2003; 171:2896–2903. [PubMed: 12960312]
39. Kim EH, et al. Signal integration by Akt regulates CD8 T cell effector and memory differentiation. J Immunol. 2012; 188:4305–4314. [PubMed: 22467649]
40. Macintyre AN, et al. Protein kinase B controls transcriptional programs that direct cytotoxic T cell fate but is dispensable for T cell metabolism. Immunity. 2011; 34:224–236. [PubMed: 21295499]
41. Ciofani M, Zuniga-Pflucker JC. Notch promotes survival of pre-T cells at the beta-selection checkpoint by regulating cellular metabolism. Nat Immunol. 2005; 6:881–888. [PubMed: 16056227]
42. Palomero T, et al. Mutational loss of PTEN induces resistance to NOTCH1 inhibition in T-cell leukemia. Nat Med. 2007; 13:1203–1210. [PubMed: 17873882]
43. Amsen D, et al. Instruction of distinct CD4 T helper cell fates by different notch ligands on antigen-presenting cells. Cell. 2004; 117:515–526. [PubMed: 15137944]
44. Ito T, et al. The critical role of Notch ligand Delta-like 1 in the pathogenesis of influenza A virus (H1N1) infection. PLoS Pathog. 2011; 7:e1002341. [PubMed: 22072963]
45. Chastagner P, Israel A, Brou C. AIP4/Itch regulates Notch receptor degradation in the absence of ligand. PLoS One. 2008; 3:e2735. [PubMed: 18628966]
46. Koo BK, et al. Mind bomb 1 is essential for generating functional Notch ligands to activate Notch. Development. 2005; 132:3459–3470. [PubMed: 16000382]
47. Guruharsha KG, Kankel MW, Artavanis-Tsakonas S. The Notch signalling system: recent insights into the complexity of a conserved pathway. Nat Rev Genet. 2012; 13:654–666. [PubMed: 22868267]
48. Demarest RM, Ratti F, Capobianco AJ. It's T-ALL about Notch. Oncogene. 2008; 27:5082–5091. [PubMed: 18758476]
49. Cantrell D. Protein kinase B (Akt) regulation and function in T lymphocytes. Semin Immunol. 2002; 14:19–26. [PubMed: 11884227]

50. Hand TW, et al. Differential effects of STAT5 and PI3K/AKT signaling on effector and memory CD8 T-cell survival. Proceedings of the National Academy of Sciences of the United States of America. 2010; 107:16601–16606. [PubMed: 20823247]

51. Pipkin ME, et al. Interleukin-2 and inflammation induce distinct transcriptional programs that promote the differentiation of effector cytolytic T cells. Immunity. 2010; 32:79–90. [PubMed: 20096607]

52. Finlay DK, et al. PDK1 regulation of mTOR and hypoxia-inducible factor 1 integrate metabolism and migration of CD8+ T cells. J Exp Med. 2012; 209:2441–2453. [PubMed: 23183047]

53. Doedens AL, et al. Hypoxia-inducible factors enhance the effector responses of CD8(+) T cells to persistent antigen. Nat Immunol. 2013; 14:1173–1182. [PubMed: 24076634]

54. Topham DJ, Castrucci MR, Wingo FS, Belz GT, Doherty PC. The role of antigen in the localization of naive, acutely activated, and memory CD8(+) T cells to the lung during influenza pneumonia. J Immunol. 2001; 167:6983–6990. [PubMed: 11739518]

55. Mueller SN, Langley WA, Carnero E, Garcia-Sastre A, Ahmed R. Immunization with live attenuated influenza viruses that express altered NS1 proteins results in potent and protective memory CD8+ T-cell responses. J Virol. 2010; 84:1847–1855. [PubMed: 19939929]

56. van der Sluijs KF, et al. IL-0 is an important mediator of the enhanced susceptibility to pneumococcal pneumonia after influenza infection. J Immunol. 2004; 172:7603–7609. [PubMed: 15187140]

57. Palmer, DF.; Dowdle, WR.; Coleman, MT.; Schild, GC. Advanced laboratory techniques for influenza diagnosis: procedural guide. Haemagglutination inhibition test, in Atlanta: US Department of Health, Education and Welfare, Public Health Service. US Department of Health, Education and Welfare, Public Health Service; 1975. p. 25-62.

58. Anders S, et al. Count-based differential expression analysis of RNA sequencing data using R and Bioconductor. Nat Protoc. 2013; 8:1765–1786. [PubMed: 23975260]

59. Young MD, Wakefield MJ, Smyth GK, Oshlack A. Gene ontology analysis for RNA-seq: accounting for selection bias. Genome biology. 2010; 11:R14. [PubMed: 20132535]

60. Isserlin R, et al. Pathway analysis of dilated cardiomyopathy using global proteomic profiling and enrichment maps. Proteomics. 2010; 10:1316–1327. [PubMed: 20127684]

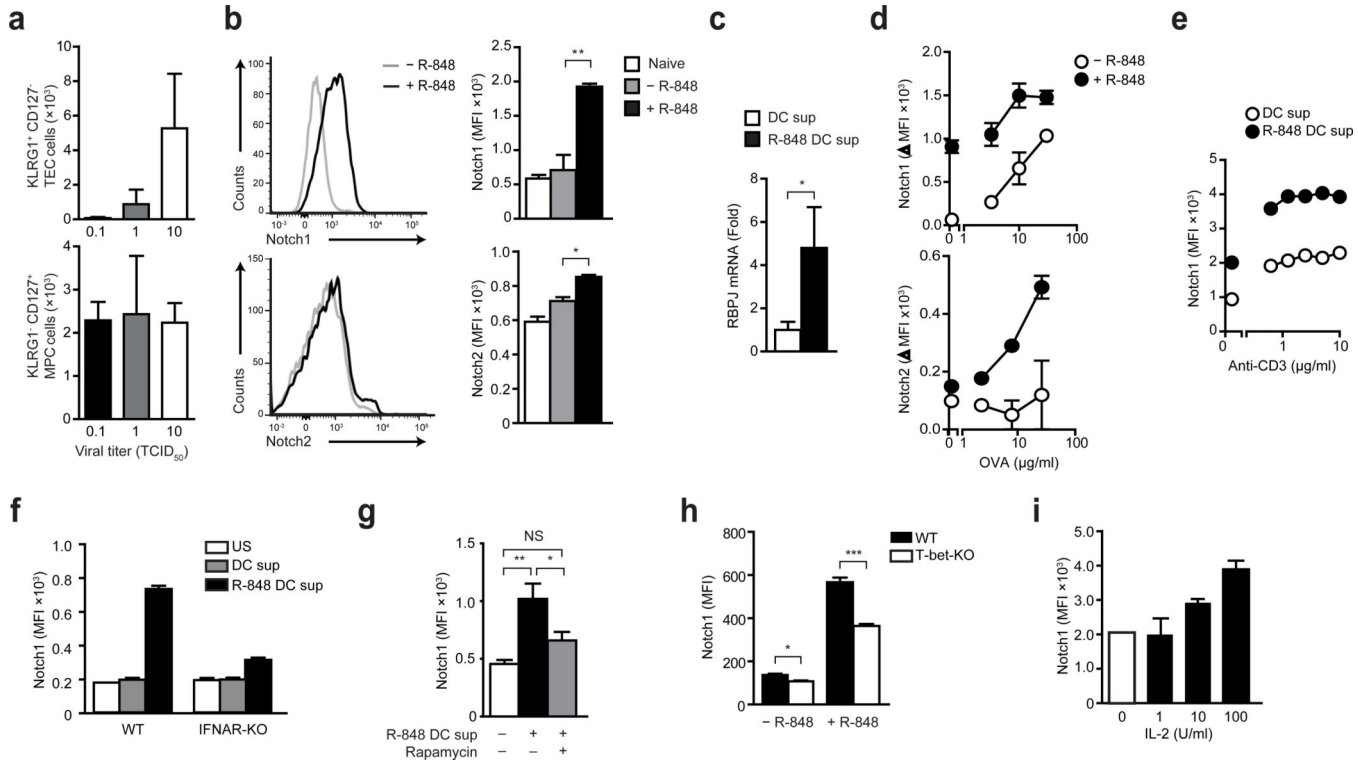

Figure 1.

TEC promoting signals induce Notch on CD8$^+$ T cells. (**a**) KLRG1$^+$CD127$^-$ (top) and KLRG1$^-$CD127$^+$ (bottom) H-2 D^b–NP$^+$CD8$^+$ T cell numbers in spleens of mice infected with different doses of A/HK×31 10 days earlier (3 mice/group). (**b**) Expression (MFI) of Notch1 (top) and Notch2 (bottom) on naïve CD8$^+$ T cells (white bars) or after 16h co-culture with BM-DC with (black bars, black histograms) or without R-848 (grey bars, grey histograms)(triplicates) (**c**) *Rbpj* mRNA expression (relative to *Actb*) in CD8$^+$ T cells stimulated o/n with anti-CD3 and control (white bar) or R-848 DC sup (black bar) (cumulative of 2 experiments, each in duplicate). (**d**) Notch1 (top) and 2 (bottom) expression on OT-I CD8$^+$ T cells activated o/n by BMDC and Ovalbumin without (white circles) or with (black circles) R-848. Isotype control staining was subtracted (ΔMFI) (duplicates). (**e–i**) Notch1 expression on (**e**) CD8$^+$ T cells stimulated o/n with anti-CD3 and control (white circles) or R-848 DC sup (black circles) (duplicates), (**f**) wild-type and type I IFN receptor knock-out (IFNAR1ko) CD8$^+$ T cells, unstimulated (US-white bars) or stimulated with control (grey bars) or R-848 DC sup (black bars) (duplicates), (**g**) CD8$^+$ T cells, unstimulated (white bar) or stimulated as in (**f**) with (grey bars) or without Rapamycin (black bars) (3 to 6 replicates/group), (**h**) wild-type (black bars) or *Tbx21*$^{-/-}$ CD8$^+$ T cells stimulated as in (c) (triplicates), (**i**) CD8$^+$ T cells stimulated with anti-CD3 and IL-2 (duplicates and quadruplicates). (**a,f,h,i**) representative of two ,(**d,e,g**) of three and (**b**) of more than five experiments. Mean + s.e.m. *P < 0.05; **P < 0.01; ***P < 0.001, two-tailed *t*-test or one-way ANOVA with Bonferroni corrections.

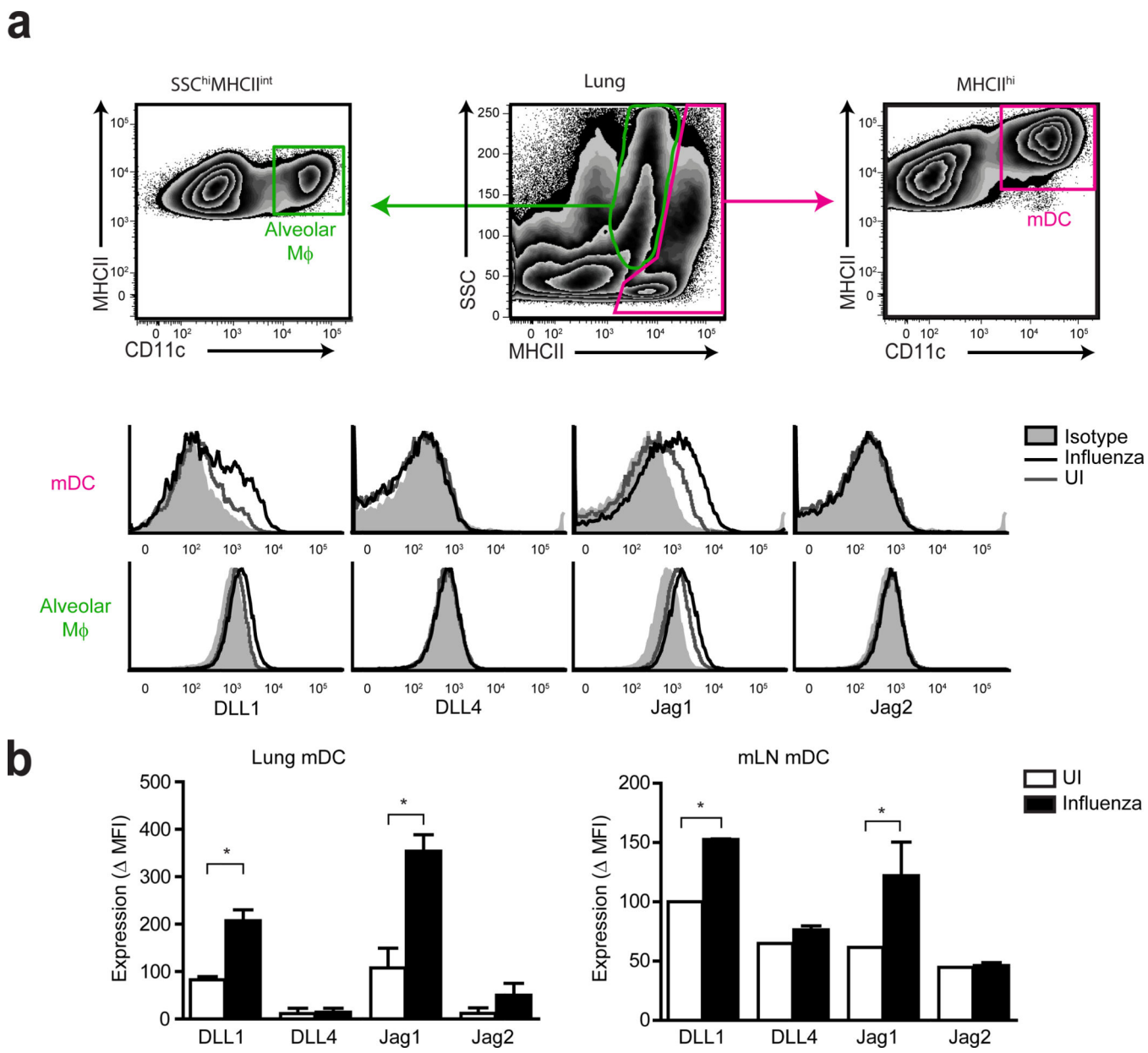

Figure 2.

Notch ligands are expressed on APC during influenza infection. C57BL/6 mice were infected intranasally with A/HK×31 influenza. (**a**) Five days post infection (p.i.) expression of DLL1, DLL4, Jagged1 and Jagged2 expression on lung APC subsets was measured by flow cytometry. Two main APC subsets in the lung were defined as mDCs (migratory DC, $MHCII^{hi}CD11c^{hi}$, red gate) or macrophages (Alveolar Mf, $SSC^{hi}MHCII^{int}CD11c^{hi}$, green gate). Filled histograms represent staining with isotype control mAb (Isotype co.), grey lines show Notch ligand expression on APC isolated from non-infected lungs (Uninfected co.), and black lines indicate expression on APC isolated from infected lungs (influenza infected). (**b**) Mean Fluorescence Intensity of DLL1, DLL4, Jagged1 and Jagged2 on mDC isolated from the lung (left) or isolated from the draining mLN (right). Shown is Δ-MFI (corrected

for background staining with isotype control mAb) for non-infected (white bars) and infected mice (black bars). Results represent 2 (uninfected) or 4 (infected) separately processed mice from a representative of 5 experiments. Mean + s.e.m. *P < 0.05, two-tailed *t*-test.

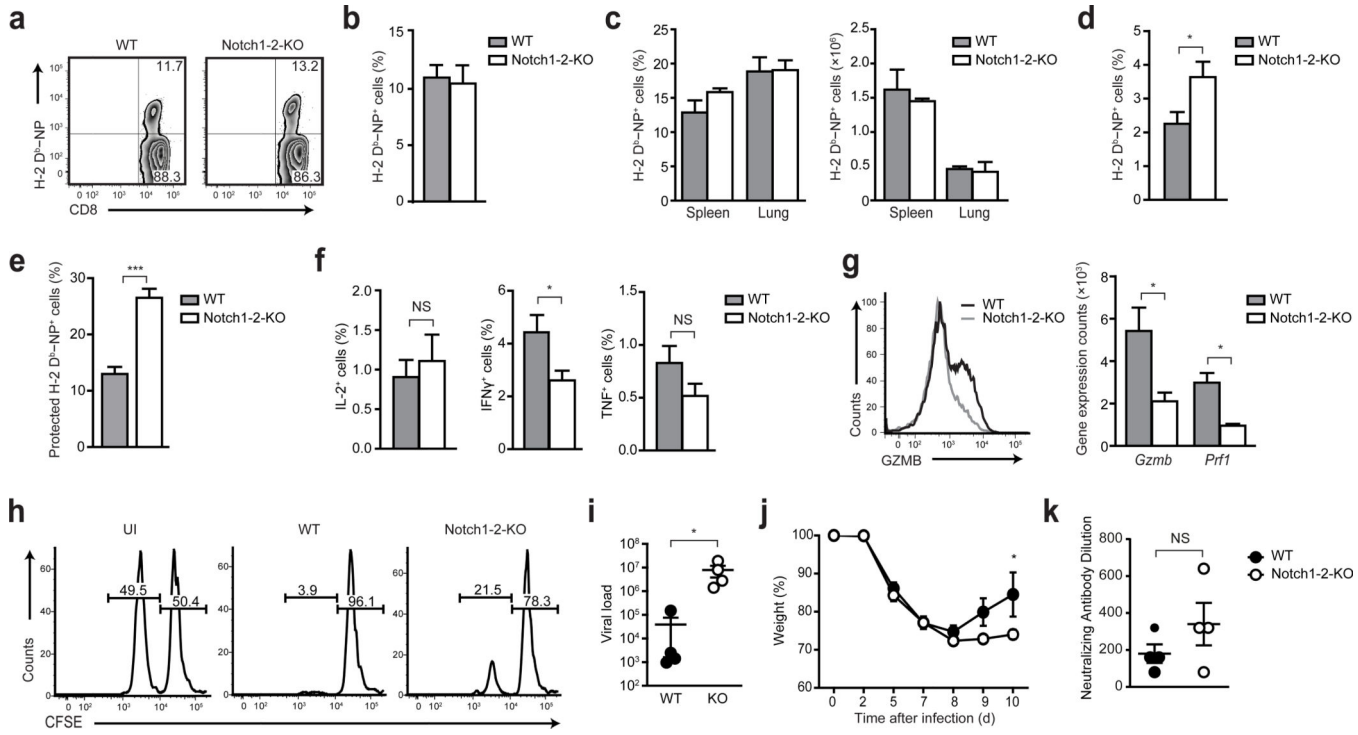

Figure 3.

Notch is required for effector function. Mice were infected with A/HK×31 and analyzed after 10 days. (**a**) Flow cytometry profiles and (**b**) frequencies of H-2 D^b–NP^+ cells of $CD8^+$ T cells in blood from (15) WT (grey bars) and (10) Notch1-2-KO (white bars) mice (3 pooled experiments). (**c**) Frequencies (left) and numbers (right) of H-2 D^b–NP^+ cells of $CD8^+$ T cells in spleens and lungs (2 mice per genotype, representative of over 10 experiments), or (**d**) mediastinal LN (10 wild-type and 11 Notch1-2-KO mice/group from 3 experiments). (**e**) Percentage H-2 D^b–NP^+ of $CD8^+$ T cells in spleens unstained by intravenous anti-CD8 (11 mice/group from 3 experiments). (**f**) Percentages $NP_{366–374}$ stimulated lung $CD8^+$ T cells producing IL-2, IFN-γ and TNF (14 or 15 mice/genotype from 4 experiments) or (**g**) Granzyme-B (WT-black line; Notch1-2-KO-grey line) (representative of 4 experiments, minimally 3 mice/group). (right) Granzyme B (*Gzmb*) and perforin (*Prf1*) mRNA in splenic H-2 D^b–NP^+CD8^+ T cells (RNAseq-average expression of 3 experiments, each 3 pooled mice/group). (**h**) *In vivo* cytolysis assay. Uninfected (UI-left) or A/HK×31 infected (10 days earlier) WT (middle) or Notch1-2-KO mice (right) were injected with syngeneic splenocytes labeled with $NP_{366–374}$ peptide and low CFSE or without peptide and high CFSE (1:1 ratio). Numbers represent percentage of cells per CFSE peak in spleens 4h after injection (representative of 4 mice/group). (**i–k**) 10 days after 200x$TCID_{50}$ A/PR/8/34 infection. Symbols represent individual mice (closed-WT; open-Notch1-2-KO). (**i**) Lung viral loads. (**j**) Relative weights (normalized to day 0) day 0–7 n=12; day 8 n=8; day 9–10 n=4. (**k**) Neutralizing antibodies to A/PR/8/34 in sera. Mean + s.e.m. *P < 0.05; **P < 0.01, (**d,e,f**) two-tailed *t*-test; 2-tailed Mann Whitney test (**i,k**); two-way ANOVA, Sidak's multiple comparisons test (**j**)).

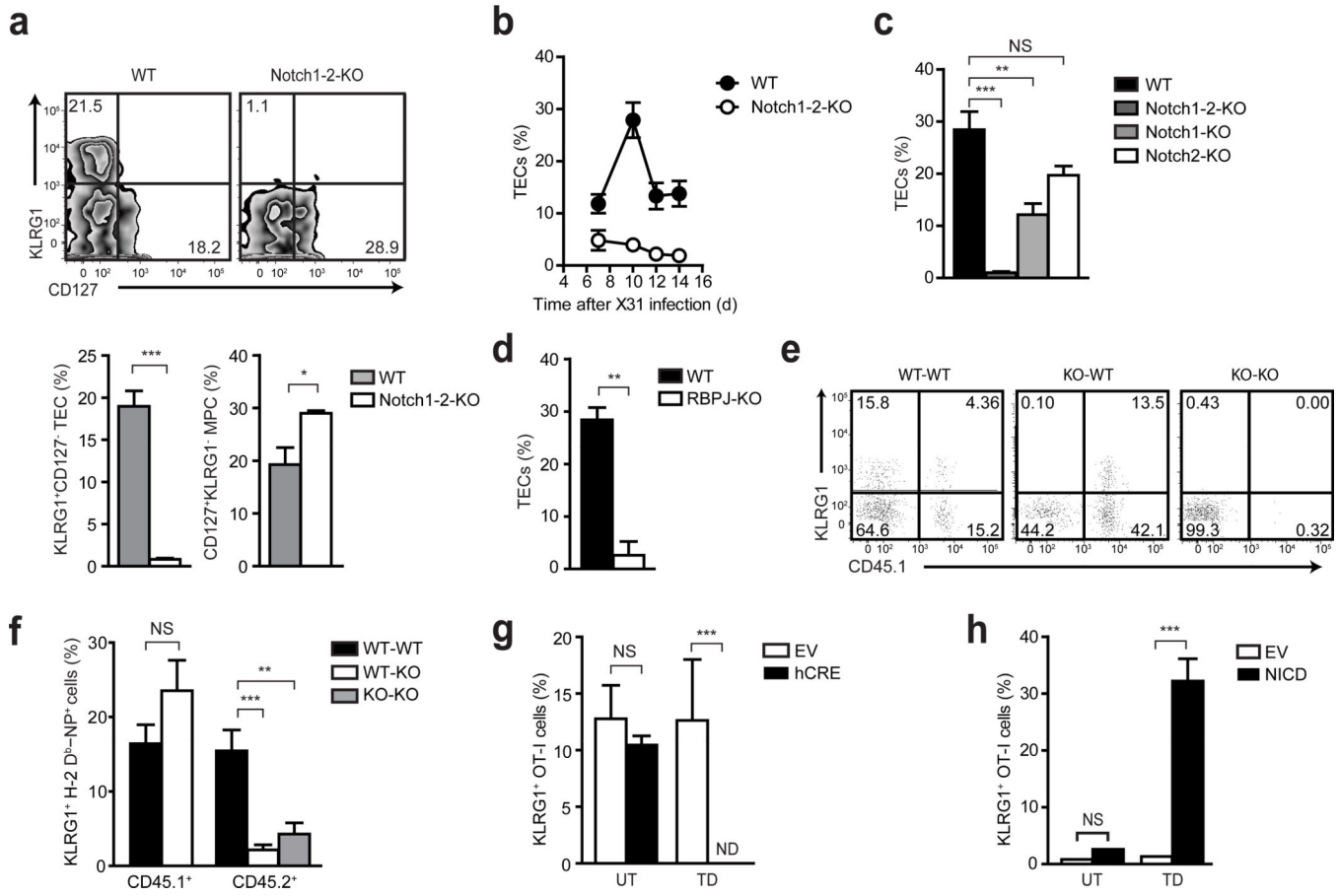

Figure 4.

Notch is required for TEC differentiation. (**a–f**) Mice were infected with A/HK×31. (**a**) Flow cytometry plots for KLRG1 and CD127 on splenic H-2 D^b–NP^+CD8^+ T cells after 10 days. (bottom) average frequencies $KLRG1^+CD127^-$ TECs (left) and $KLRG1^-CD127^+$ MPCs (right) of $CD8^+$ T cells (WT-grey bars; Notch1-2-KO -white bars) (3 mice/group). (**b**) Time course percentages $CD127^-$ $KLRG1^+$ TECs among H-2 D^b–NP^+CD8^+ T cells in blood (closed symbols-WT; open symbols- Notch1-2-KO) (3 to 20 mice per data point). (**c**) Percentages $KLRG1^+CD127^-$ TECs in blood of wild-type (black bar), Notch1-2-KO (dark grey bar), Notch1 (light grey bar) or Notch2 (white bar) single knockout mice (minimally 6 mice/group from 3 experiments) or (**d**) RBPJ knockout mice, 10 days after infection (3 mice/group). (**e,f**) Mixed chimeras of $CD45.1^+$ WT + $CD45.2^+$ WT (left) or $CD45.1^+$ WT + $CD45.2^+$ Notch1-2-KO bone marrow were made and analyzed 10 days after infection. (**e**) CD45.1 versus KLRG1 on H-2 D^b–NP^+CD8^+ T cells. (**f**) Percentages $KLRG1^+$ H-2 D^b–NP^+CD8^+ T cells (black bars-$CD45.1^+$ WT with $CD45.2^+$ WT; white bars-$CD45.1^+$ WT with $CD45.2^+$ Notch1-2-KO; grey bar-CD45.2 Notch1-2-KO) (8 or more mice/group from 3 experiments). (**g**) Percentages $KLRG1^+$ OT-I T cells from *Notch1*$^{flox/flox}$*Notch2*$^{flox/flox}$ mice, expressing control (white bars) or hCre (black bars) retrovirus, 5 days after transfer into OVA-influenza infected mice. Untransduced (UT) and transduced (TD) T cells from the same cultures are shown (3 mice/group). (**h**) Percentages $KLRG1^+$ Notch1-2-KO OT-I T cells, expressing control (white bars-EV) or NICD1 (black bars) retrovirus, 5 days after

transfer into OVA-influenza infected mice (2 mice per group). Mean + s.e.m. *P < 0.05; **P < 0.01; ***P < 0.001, two-tailed *t*-test or one-way ANOVA with Bonferroni corrections. (**d**) representative of two, (**e,g,h**) of three and (**a**) of more than ten experiments.

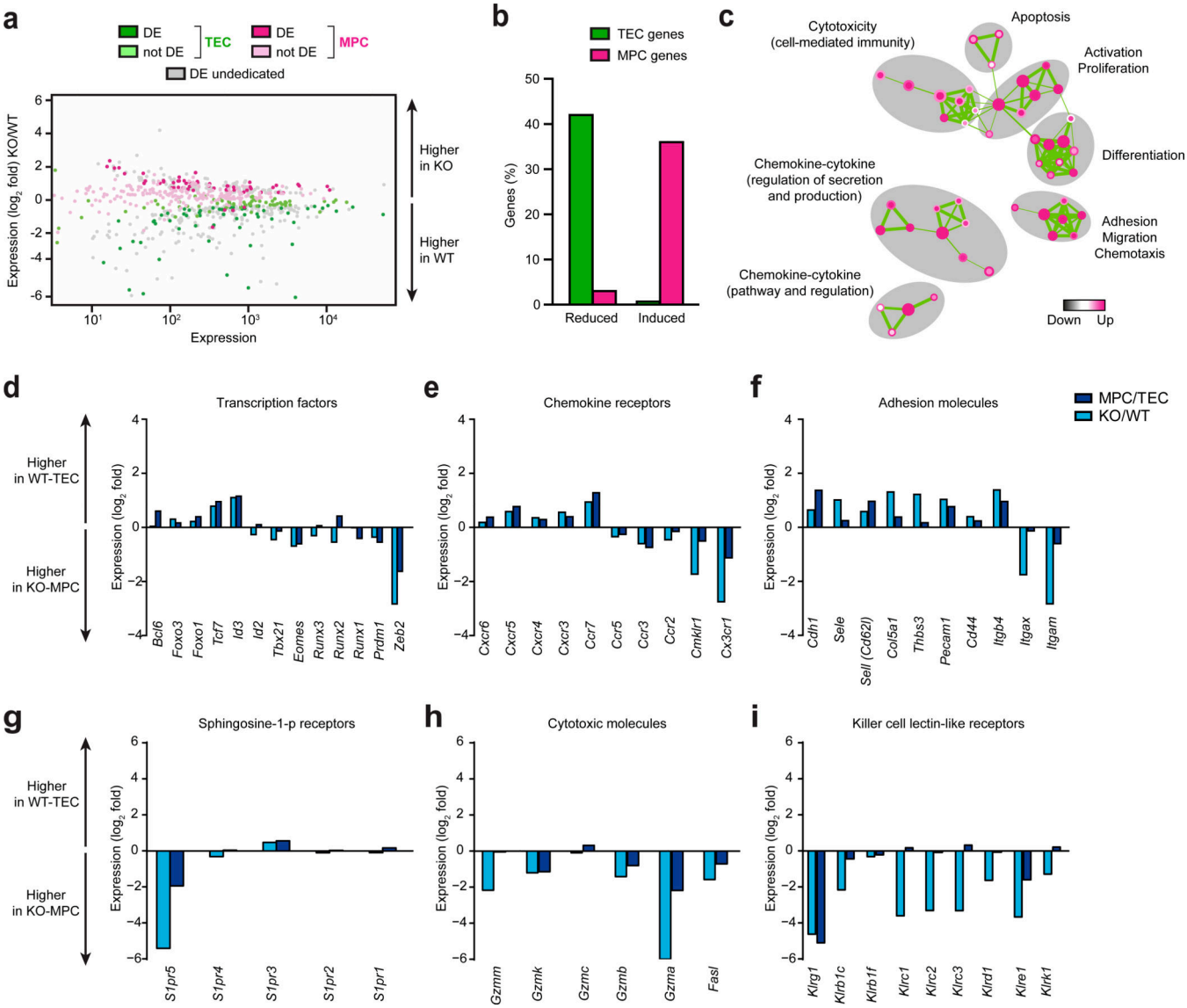

Figure 5.

Notch regulates the TEC transcriptome. RNAseq was performed on splenic H-2 D^b–NP^+CD8^+ T cells from WT and Notch1-2-KO mice 10 days post-infection with A/HK×31. (**a**) Mean expression versus log_2FoldChange (Notch1-2-KO/wild-type) plot of differentially expressed (DE) genes. TEC-(green) and MPC-specific genes (magenta) were determined by RNAseq of $CD8^+$ H-2 D^b–NP^+ $KLRG1^+CD127^-$ TECs and $KLRG1^-CD127^+$ MPCs from WT mice (Supplementary dataset 2). Grey, magenta and green dots represent significantly (adjusted *P*-value < 0.05) DE genes comparing WT versus Notch1-2-KO. Also shown are TEC- or MPC-specific genes not significantly DE between wild-type and Notch1-2-KO (light colored dots). (**b**) Percentages of TEC-specific (green bars) or MPC-specific genes (magenta bars), significantly (*padj*<0.05) reduced (left) or induced (right) in Notch1-2-KO H-2 D^b–NP^+CD8^+ T cells. (**c**) GSEA Enrichment Map (using GO terms for Biological Pathways-see Supplementary dataset 3 for enriched GO-terms). Node core and periphery represent gene set enrichment in the comparison of Notch1-2-KO versus WT (core) or MPC

versus TEC (periphery). Node color represents significance of enrichment (magenta-enriched, white-not enriched). Connecting line length represents similarity between gene sets and thickness the number of genes shared. DE genes with an FDR of <0.5 were selected for GSEA. Gene categories shown are enriched at an FDR<0.1. (**d–i**) Log_2-fold ratio of expression between MPC/TEC (dark blue bars) and Notch1-2-KO/WT (light blue bars) for (**d**) transcription factors, (**e**) chemokine receptors, (**f**) adhesion molecules, (**g**) S1PR family members, (**h**) cytolytic effector molecules and (**i**) killer cell lectin-like Receptor genes. (**e,f**) restricted to genes with minimally 2-fold difference between MPC vs TEC or Notch1-2-KO vs WT (note: CD44 and Sell included for completion). RNAseq data available at Array Express (E-MTAB-2255). Cumulative from 3 experiments, each with 3 pooled mice/ genotype.

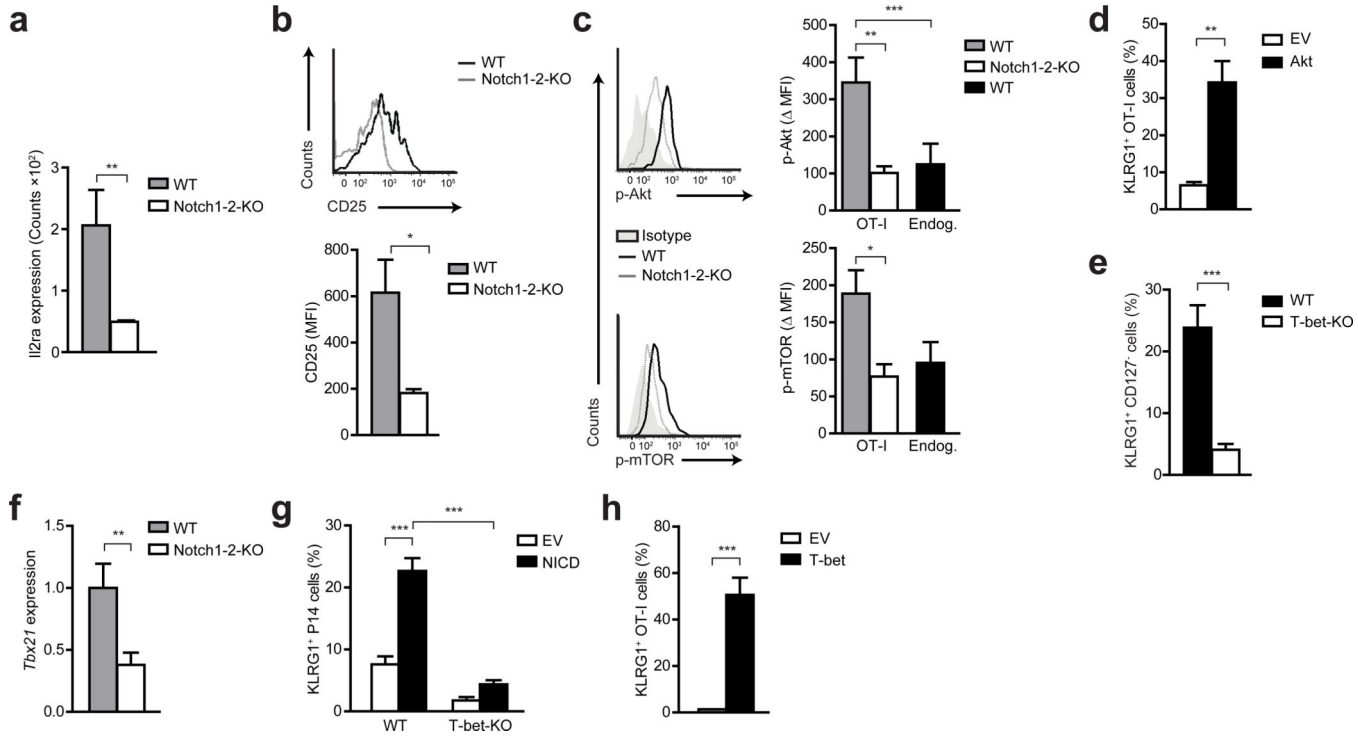

Figure 6.

Notch regulates pathways controlling TEC differentiation. (**a**) *Il2rα* mRNA in WT (grey bar) and Notch1-2-KO (white bar) cells determined as in Figure 5. (**b**) CD25 surface profile (top) and average MFI (7 mice/group, from 2 experiments) on transferred wild-type (black line, grey bar) or Notch1-2-KO (grey line, white bar) OT-I CD8$^+$ T cells, 5 days post-infection with OVA-influenza. (**c**) Flow cytometry profiles (left) and average ΔMFI (right-isotype control background subtracted) for phosphorylated AKT (T308) and mTOR (S2448) in transferred wild-type (black line, grey bars) and Notch1-2-KO (grey line, white bars) OT-I T cells or endogenous CD44$^-$CD8$^+$ T cells (black bars), 5 days post-infection with OVA-influenza (pooled from 6 mice/group, 2 experiments, representative of 3). (**d**) KLRG1 expression on Notch1-2-KO OT-I T cells expressing control (white bars) or myr-AKT (black bars) IRES-GFP retrovirus, 5 days after transfer into OVA-influenza infected mice. Minimally 5 mice/group, 2 pooled experiments. (**e**) Percentages KLRG1$^+$CD127$^-$ TECs in blood of wild-type (black bar) and *Tbx21*$^{-/-}$ (white bar) mice, 10 days after A/HK×31 infection (minimally 7 mice/genotype). (**f**) *Tbx21* mRNA expression (relative to *Actb*) in wild-type (grey bar) or Notch1-2-KO (white bar) splenic H-2 Db–NP$^+$CD8$^+$ T cells, 10 days after A/HK×31 infection (4 mice/group, 2 experiments). (**g**) KLRG1 expression on wild-type (left) and *Tbx21*$^{-/-}$ (right) P14 T cells, expressing control (white bars) or NICD1 (black bars) IRES-GFP retrovirus, 5 days after transfer into gp$_{33–41}$-influenza infected mice (minimally 5 mice per group, 2 experiments). (**h**) KLRG1 expression on Notch1-2-KO OT-I T cells, expressing control (white bars) or T-bet (black bars) encoding retrovirus, analyzed as in (g) (2 mice/genotype, representative experiment of 3). Shown is the mean + s.e.m. *P < 0.05; **P < 0.01; ***P < 0.001; unpaired, two-tailed *t*-test or One-way ANOVA with Bonferroni corrections.